

The Role of Nucleons in Electromagnetic Emission Rates

James V. Steele¹ and Ismail Zahed²

¹*Department of Physics, The Ohio State University, Columbus, OH 43210, USA*

²*Department of Physics and Astronomy, SUNY, Stony Brook, NY 11794, USA*

(February 8, 1999)

Abstract

Electromagnetic emission rates from a thermalized hadronic gas are important for the interpretation of dilepton signals from heavy-ion collisions. Although there is a consensus in the literature about rates for a pure meson gas, qualitative differences appear with a finite baryon density. We show this to be essentially due to the way in which the πN background is treated in regards to the nucleon resonances. Using a background constrained by unitarity and broken chiral symmetry, it is emphasized that the thermalized hadronic gas can be considered dilute.

PACS numbers: 25.75.-q 12.38.Lg 11.30.Rd 11.40.Ha

arXiv:hep-ph/9901385v2 8 Feb 1999

Recent relativistic heavy-ion collisions at CERN have reported an excess of dileptons over a broad range of invariant mass $M = 300\text{-}500$ MeV [1,2]. Various theoretical assessments of the dilepton emission rates have tried to understand this excess. In the absence of baryons, the rates achieved using detailed reaction processes [3,4] and spectral sum rules [5,6] agree with each other, but fail to reproduce the enhancement in the data. In the presence of baryons, calculations using many-body dynamics [7,8] lead to larger rates below the ρ peak compared to results from spectral considerations constrained by broken chiral symmetry [9].

This is illustrated by the left plot of Fig. 1 for pertinent temperature $T = 150$ MeV and baryon chemical potential¹ $\mu = 520$ MeV. Although neither rate accommodates the data in a realistic hydrodynamical evolution [10], the rates from Ref. [7,8] are about two to three times larger than those of Ref. [9], being within only two standard deviations of the data. We show below that the discrepancy between these two rates originates chiefly from the πN background, and that the hadronic gas is essentially dilute, in confirmation of our earlier work [9].

Although perturbative unitarity fixes the πN background uniquely in the Compton amplitude, its extrapolation away from the photon-point requires care. In Ref. [9] this extrapolation was implemented by paying due care to threshold unitarity. In the future, the complicated issue of background versus resonances should be properly resolved by enlarging the theoretical analysis to pion photo-production as well as pion knock-out while obeying unitarity and broken chiral symmetry as detailed in Ref. [11]. For now, we concentrate on illuminating the reason for the above differences in the two theoretical estimates containing nucleons.

In a thermal equilibrated hadronic gas, the rate \mathbf{R} of dileptons produced in an unit four volume follows from the thermal expectation value of the electromagnetic current-current correlation function [12]. For massless leptons with momenta p_1 and p_2 , the rate per unit invariant momentum $q = p_1 + p_2$ is given by [9]

$$\frac{d\mathbf{R}}{d^4q} = -\frac{\alpha^2}{3\pi^3 q^2} \frac{1}{1 + e^{q^0/T}} \text{Im}\mathbf{W}^F(q) \quad (1)$$

where $\alpha = e^2/4\pi$ is the fine structure constant, and

$$\mathbf{W}^F(q) = i \int d^4x e^{iq \cdot x} \text{Tr} \left(e^{-(\mathbf{H} - \mu \mathbf{N} - \Omega)/T} T^* \mathbf{J}^\mu(x) \mathbf{J}_\mu(0) \right). \quad (2)$$

$e\mathbf{J}_\mu$ is the hadronic part of the electromagnetic current, \mathbf{H} is the hadronic Hamiltonian, μ is the baryon chemical potential, \mathbf{N} is the baryon number operator, Ω is the Gibbs energy, T is the temperature, and the trace is over a complete set of hadron states.

We expand the trace in Eq. (2) using pion and nucleon states. This is justified for temperatures $T \lesssim m_\pi$ and final nucleon densities $\rho_N \lesssim 3\rho_0$ with $\rho_0 = 0.16 \text{ fm}^{-3}$, since the

¹ We express our rates using a complete set of stable states [9] and therefore μ refers solely to nucleons. In the analysis of Ref. [7,8], μ refers to all possible baryons as they retain the unstable particles in their final states. The rate comparison done here is only meaningful for fixed T and μ .

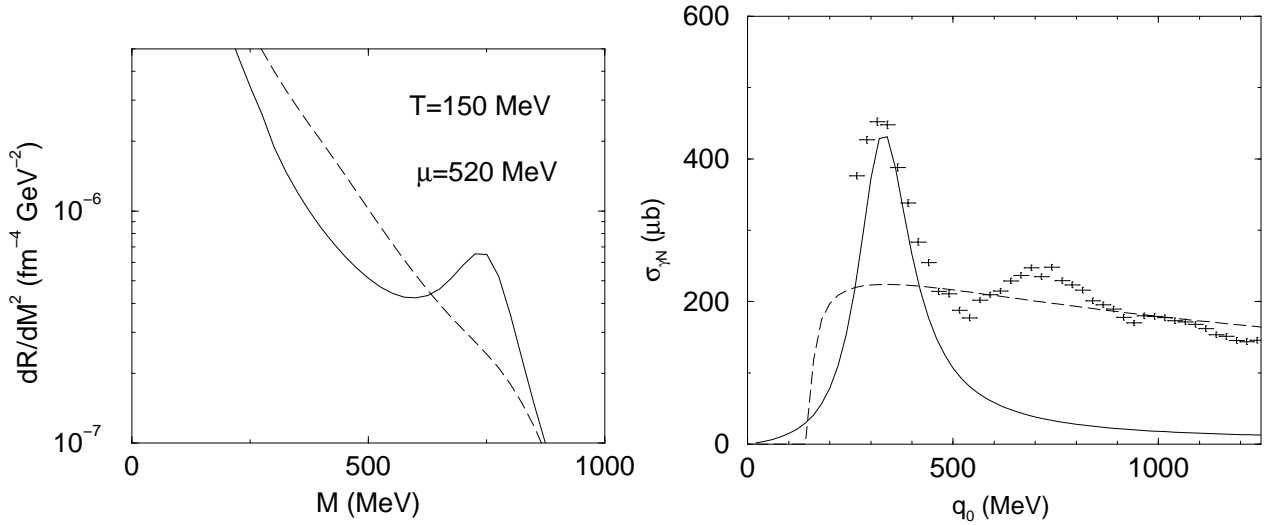


FIG. 1. The left plot compares nucleon rates from Refs. [9] (solid) and [7] (dashed). The right plot shows the results for the (isospin averaged) Compton scattering on the nucleon from the Δ (solid) and background (dashed) versus data [13].

relevant expansion parameter κ for each particle is less than $\frac{1}{3}$ in that regime. This allows us to only retain terms up to first order in density [9]

$$\text{Im } \mathbf{W}^F(q) = -3q^2 \text{Im } \mathbf{\Pi}_V(q^2) + \frac{1}{f_\pi^2} \int d\pi \mathbf{W}_\pi^F(q, k) + \int dN \mathbf{W}_N^F(q, p) + \mathcal{O}(\kappa_\pi^2, \kappa_N^2, \kappa_\pi \kappa_N). \quad (3)$$

The phase space factors are

$$dN = \frac{d^3p}{(2\pi)^3} \frac{1}{2E_p} \frac{1}{e^{(E_p - \mu)/T} + 1} \quad \text{and} \quad d\pi = \frac{d^3k}{(2\pi)^3} \frac{1}{2\omega_k} \frac{1}{e^{\omega_k/T} - 1},$$

with nucleon energy $E_p = \sqrt{m^2 + p^2}$ and pion energy $\omega_k = \sqrt{m_\pi^2 + k^2}$. The first term in Eq. (3) is the transverse part of the isovector correlator $\langle 0|T^* \mathbf{V}\mathbf{V}|0\rangle$ and summarizes the results of the resonance gas model. It is given by e^+e^- annihilation data. At low and moderate q^2 this is dominated by the ρ and ρ' while at high q^2 its tail is determined by the $q\bar{q}$ spectrum.

The term linear in pion density can be expressed in terms of experimentally measurable quantities by use of chiral reduction formulas. The important contributions are [5]

$$\begin{aligned} \mathbf{W}_\pi^F(q, k) \simeq & 12q^2 \text{Im } \mathbf{\Pi}_V(q^2) - 6(k+q)^2 \text{Im } \mathbf{\Pi}_A((k+q)^2) + (q \rightarrow -q) \\ & + 8((k \cdot q)^2 - m_\pi^2 q^2) \text{Im } \mathbf{\Pi}_V(q^2) \text{Re}(\Delta_R(k+q) + \Delta_R(k-q)) \end{aligned} \quad (4)$$

with $\Delta_R(k)$ the retarded pion propagator and $\mathbf{\Pi}_A$ the transverse part of the iso-axial correlator $\langle 0|T^* \mathbf{j}_A \mathbf{j}_A|0\rangle$ which follows from tau decay data [5]. It is dominated by the a_1 resonance.

The term linear in nucleon density is just the spin-averaged forward Compton scattering amplitude on the nucleon with virtual photons. This is only measured for various values of

$q^2 \leq 0$. However, the dilepton and photon rates require $q^2 \geq 0$. Therefore, only the photon rate for this term can be determined directly from data by use of the optical theorem

$$e^2 \mathbf{W}_N^F(q, p) = -4(s - m^2) \sum_I \sigma_{\gamma N}(s) \quad (5)$$

with $s = (p + q)^2$. For off-shell photons, we must resort to chiral constraints to determine the nucleon contribution to the dilepton rate. Broken chiral symmetry dictates uniquely the form of the strong interaction Lagrangian (at tree level) for spin- $\frac{1}{2}$ particles. Perturbative unitarity follows from an on-shell loop-expansion in $1/f_\pi$ that enforces current conservation and crossing symmetry. To one-loop, the πN contribution is parameter free. The large contribution of the Δ to the Compton amplitude near threshold is readily taken into account by adding it as a unitarized tree term to the one-loop result [9]. The result for Compton scattering on the nucleon from Ref. [9] is shown in the right plot of Fig. 1 versus data [13].

This fit to the Compton data is good, given the fact it is a parameter-free analysis. However, we must determine the role of the $N^*(1520)$, since about 20% of the cross section is unaccounted for in that kinematic region. More importantly, it has been suggested that the decay of this resonance in matter is what feeds the dilepton rate enhancement [7,8]. We note that the $N^*(1520)$ has about a 50% branching ratio to the πN channel, making it difficult to disentangle from the πN background.

The contribution of the $N^*(1520)$ to the Compton amplitude follows readily from the transition matrix element

$$\begin{aligned} \langle N(p) | \mathbf{J}_\mu | N^*(k) \rangle = \bar{u}(p) & \left[Q_*(q^2) (\gamma_\mu q_\nu - g_{\mu\nu} \not{q}) + i S_*(q^2) \sigma_\mu^\lambda q_\lambda q_\nu \right. \\ & \left. + \left(R_*(q^2) + \not{q} \bar{R}_*(q^2) \right) (q_\mu q_\nu - g_{\mu\nu} q^2) \right] \frac{1 + \tau^3}{2} u^\nu(k). \end{aligned} \quad (6)$$

The form factors Q_* , S_* , R_* and \bar{R}_* comprise a maximal set and are real by time reversal invariance. This decomposition parallels the one adopted for the Δ in Ref. [9] with adjustments for the difference in parity and isospin between the two resonances. Hence, the $N^*(1520)$ contribution to the Compton amplitude $\mathcal{M}_*(s, q^2)$ is the same form as $\mathcal{M}(s, q^2)$ for the Δ quoted in Ref. [9] as long as m_Δ is changed to $-m_*$ (parity) and the prefactor $\frac{4}{3}$ is changed to 1 (isospin). Just as for the Δ , the form factors in Eq. (6) will be assumed q^2 independent.

The resulting couplings are constrained by the nucleon polarizabilities, the E/M -ratio, and the Compton amplitude. The nucleon polarizabilities can be separated into the loop, Δ , and N^* contributions:

$$\bar{\alpha} + \bar{\beta} = (\bar{\alpha} + \bar{\beta})_{\text{loop}} + \frac{8\alpha}{9} \frac{m}{m_\Delta^2} \frac{m_\Delta^2 + m^2}{m_\Delta^2 - m^2} Q^2 + \frac{2\alpha}{3} \frac{m}{m_*^2} \frac{m_*^2 + m^2}{m_*^2 - m^2} Q_*^2, \quad (7)$$

$$\bar{\beta} = \bar{\beta}_{\text{loop}} + \frac{8\alpha}{9} \frac{Q^2}{m_\Delta - m} - \frac{2\alpha}{3} \frac{Q_*^2}{m_* + m}. \quad (8)$$

Note that the Δ contribution gives $E2/M1 \sim -0.3$ while empirically it is -0.015 , and the N^* contribution gives $E1/M2 \sim -3$ while empirically it is between -2 and -3 . Using that the (isospin averaged) experimental results [13] are $\frac{1}{2}(15.8 + 14.2) \times 10^{-4} \text{ fm}^3$ and

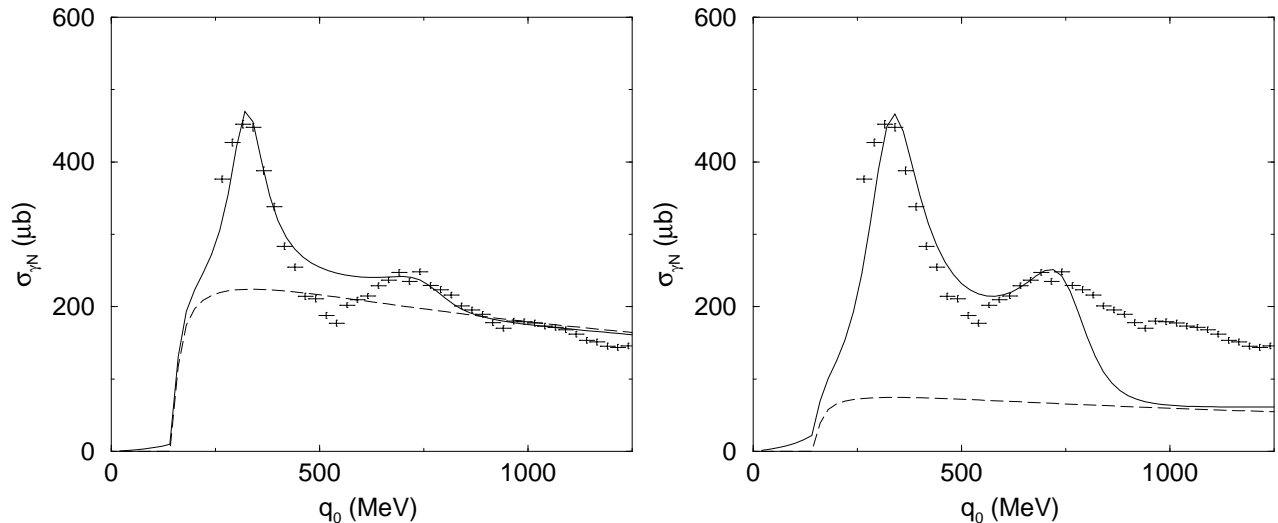


FIG. 2. Background contribution (dashed) and total contribution (solid) to the Compton amplitude compared to data [13] (crosses). The left plot is for the full background and right plot is for one-third the background.

$\frac{1}{2}(6.0 + 2.1) \times 10^{-4} \text{ fm}^3$ and the loop contributions [14] are $\frac{1}{2}(8.8 + 5.4) \times 10^{-4} \text{ fm}^3$ and $-\frac{1}{2}(1.5 + 2.2) \times 10^{-4} \text{ fm}^3$ respectively, we may estimate the values of the couplings Q and Q_* , with some freedom available from error bars. We choose² $Q = 1.8/m$ and $Q_* = 2.2/m$ for which the polarizabilities are $\bar{\alpha} + \bar{\beta} = 13 \times 10^{-4} \text{ fm}^3$ and $\bar{\beta} = 3.6 \times 10^{-4} \text{ fm}^3$.

We note that R_* and \bar{R}_* do not contribute at $q^2 = 0$, and are mainly associated with the longitudinal part of the electroproduction cross section for $q^2 < 0$. By analogy with the Δ , they will be set to zero [9]. We are therefore left to constrain S_* which is readily done by fitting to the Compton amplitude. Given the πN background, we find $S_* = -1.5/m^2$. Similarly $S = 1.5/m^2$ for the Δ offers a better fit than the value $S = 1.2/m^2$ quoted in Ref. [9]. The radiative width from the resonant part of the Δ and N^* are 0.27 MeV and 0.19 MeV respectively, to which the contribution from the πN background should be added.

The fit to the Compton amplitude resulting from this new set of parameters and including the πN and Δ background is shown in the left plot of Fig. 2. The background contribution is shown by the dashed line and the total contribution by the solid line. The crosses are the data [13]. The difference with Ref. [9] is a change in the Δ couplings (see above) to fit the data and the addition of the N^* to account for the 20% discrepancy. The background is parameter free.

To assess the importance of the πN background versus the N^* resonance in the electromagnetic emission rates, it is useful to do the following exercise: we drop the background

²The value of $Q = 2.75$ fixed purely from the Δ as quoted in Ref. [9] leads to an overestimation of the Compton cross section when added to the background, as seen in the right plot of Fig. 1. This comes from a double counting indicative of a treatment without the proper unitarization of the background and resonances.

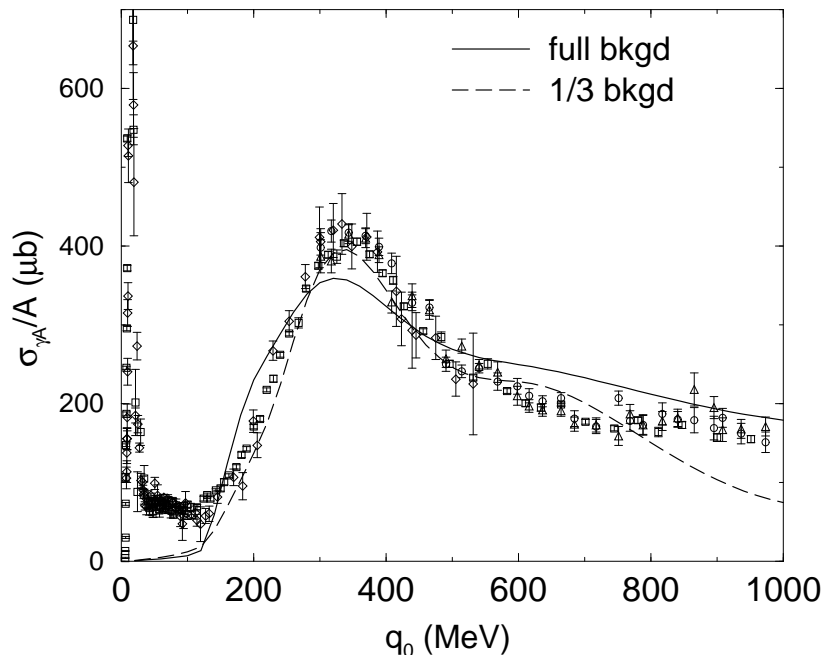


FIG. 3. Compton amplitude on nuclei comparing the two background choices to data [15].

by a factor of three and change the Δ and N^* parameters to recover the Compton amplitude, at least through the N^* region. This leads to the right plot of Fig. 2, again with the background contribution shown by the dashed lines and the total contribution by the solid line. The couplings are still fit to the experimental polarizabilities in this case giving: $(Q, Q_*) = (1.8, 4.3)/m$ and $(S, S_*) = (-2.6, -3.0)/m^2$. The E/M -ratios are therefore the same as before. This smaller background is consistent with the one used in Ref. [8]. This is clearly different from our approach in which the background is first constrained by broken chiral symmetry.

The Compton amplitude on nuclei is also measurable [15]. To leading order in the nucleon density it can be readily assessed using the Compton amplitude on a single nucleon smeared by Fermi motion (ignoring Pauli blocking),

$$\frac{\sigma_{\gamma A}}{A} = \int \frac{d^3 p}{4\pi p_F^3/3} \theta(p_F - |p|) \sigma_{\gamma N}(s) \quad (9)$$

with $q^2 = 0$ and $s = m^2 + 2q_0(E_p - |p| \cos \theta_p)$ and $p_F = 265$ MeV. The results from Eq. (9) are shown in Fig. 3 versus the data [15]. The solid line follows from the left plot of Fig. 2 while the dashed line from the right plot of Fig. 2. Since we do not account for particle-hole excitations below the πN threshold, we have not reproduced the large increase near zero q_0 . This has no consequence for the dilepton rates to be discussed below. The discrepancy of the dashed curve at high q_0 follows from neglecting the higher resonances in Fig. 2. Fermi motion smears the contribution of the Δ and $N^*(1520)$ resonances more than the background. The results for the smaller background (dashed line) is in better agreement with the data, although both predictions are within one standard deviation of the data.

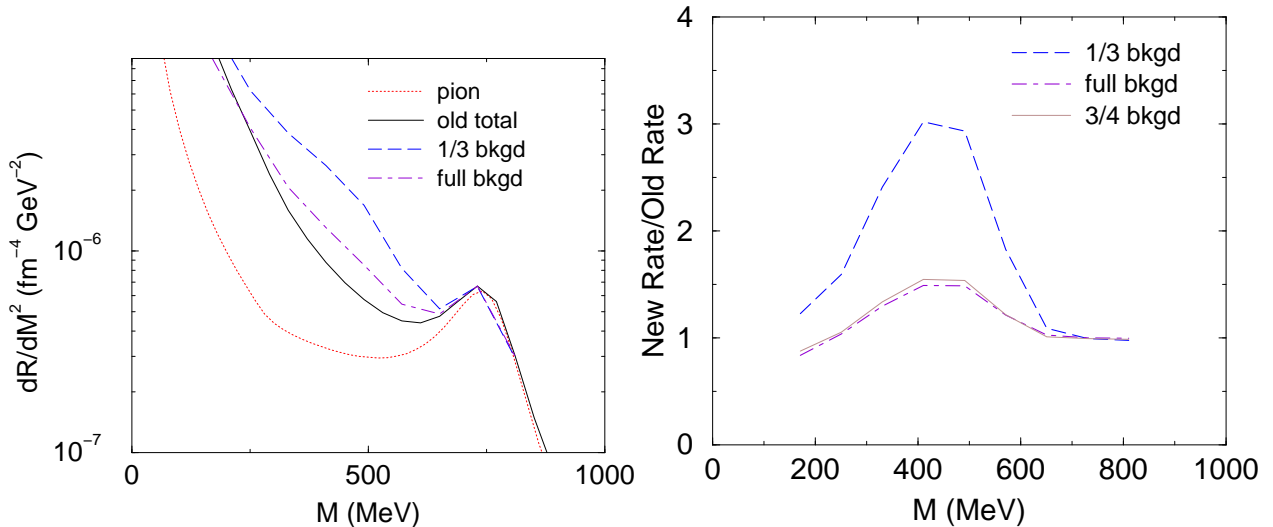


FIG. 4. The left shows the dilepton rate for $T = 150$ MeV and $\mu = 540$ MeV comparing our old result with that of the one-third background and full background. The right shows the ratio of the new results to the old result.

The nucleon contribution to the Compton amplitude as shown in Fig. 2 can be used in Eq. (3) in conjunction with the pion contribution as discussed in Ref. [9]. Using the identity ($M = \sqrt{q^2}$)

$$\frac{d\mathbf{R}}{d^4q} = \frac{2}{\pi} \frac{d\mathbf{R}}{dM^2 dy dq_{\perp}^2},$$

and integrating over rapidity y and transverse momentum q_{\perp}^2 , the dilepton rates are shown in the left plot of Fig. 4 for $T = 150$ MeV and $\mu = 540$ MeV (corresponding to a nucleon density of ρ_0). The purely pionic contribution is shown by the dotted line, the dot-dashed line is the result corresponding to the left plot of Fig. 2, while the dashed line is the result corresponding to the right plot of Fig. 2. The result quoted in Ref. [9] is shown by the solid line. As expected, the changes between the solid and dot-dashed lines are small and within expectations. More importantly, the dashed rate, following from the smaller background contribution, is substantially larger due to the enhancement caused by the additional strength of the N^* resonance³.

To make further comparison between the dilepton rates from different backgrounds, the right plot of Fig. 4 shows the ratios of the new rates to the old rate of Ref. [9]. The dot-dashed line is for the rate associated with the left plot of Fig. 2 while the dashed line is for the rate associated with the right plot of Fig. 2. It shows that in the intermediate mass range, the enhancement of the rates obtained from a smaller background [8] can be

³ There is also an additional strength from the Δ resonance, but it is significantly less.

two times more than those from a larger⁴ background [9]. The photon emission rates show similar behavior to the dilepton rates, with the smaller background giving twice as many photons as the larger one.

Medium modifications as discussed in Ref. [7,8] (and by others [16]) in addition appear to deplete the dilepton rates in the ρ region, which is qualitatively different from our rates with any background. The N^* contribution is fully within the theoretical uncertainties for our old rates as long as the full background is used. This implies that in the low mass range, the rates are well accounted for by merely a dilute gas. The discrepancy between our rates [9] and those in Ref. [7,8] around the ρ is real and may be indicative of some coherence or lack thereof. This point can be sorted out through higher resolution measurements as we suggested in Ref. [5,9].

The electromagnetic emission rates in a baryon-free gas are well established theoretically [3,5]. In a baryon-rich gas, the discrepancy between the rates reported in Ref. [9] and those in Ref. [8] is mainly due to the choice of the πN background. The Compton amplitude on the nucleon and nuclei can both accommodate either a small [8] or large [9] πN background. A calculation with a small background requires more strength in the resonances, leading to dilepton and photon rates that are about two times larger than from a large background at $T \sim m_\pi$ and $\rho_N \sim \rho_0$.

Perturbative unitarity and broken chiral symmetry uniquely specify the larger πN background. A one-loop expression for this quantity was used here. Adding more loops can alter and possibly deplete the background above the two-pion threshold. However, these corrections are chirally suppressed as evidenced by the fact that the one-loop calculation is a good approximation to the background above the resonances. A systematic understanding of how the higher order contributions enter, like through pion photon-production and pion knock-out, is still important. This can be done reliably using the framework proposed in Ref. [11], where due care is paid to unitarity and broken chiral symmetry. As always, it is important to constrain the dynamics of relativistic heavy ion collisions by broken chiral symmetry so that novel effects can be reliably assessed.

Acknowledgements

We thank our colleagues at both institutions for discussions, in particular R. Rapp for sharing some of his new calculations with us as well as the data compilation from Fig. 3. We also thank P. Huovinen for providing us with the data from Ref. [7], used in their comparative analysis [10]. We were also informed by R. Rapp that conclusions similar to ours were being reached [17]. This work was supported in part by the US DOE grant DE-FG02-88ER40388 and by the National Science Foundation under Grants No. PHY-9511923 and PHY-9258270.

⁴We have checked that an adjustment of the background to coincide with Ref. [7], which is about 75% of that used in Ref. [9], yields a ratio comparable to the full background as shown in the right plot of Fig. 4.

REFERENCES

- [1] G. Agakichiev, *et al.*, Phys. Rev. Lett. **75** (1995) 1272; Nucl. Phys. **A610** (1996) 317c.
- [2] M. Masera for the HELIOS-3 Collaboration, Nucl. Phys. **A590** (1995) 93c.
- [3] C. Gale and P. Lichard, Phys. Rep. **D49** (1994) 3338.
- [4] C. Gale, nucl-th/9706026, and references therein.
- [5] J. V. Steele, H. Yamagishi, and I. Zahed, Phys. Lett. **B384** (1997) 255;
C. H. Lee, H. Yamagishi, and I. Zahed, Phys. Rev. **C58** (1998) 2899.
- [6] Z. Huang, Phys. Lett. **B361** (1995) 131.
- [7] R. Rapp, M. Urban, M. Buballa, and J. Wambach, Phys. Lett. **B417** (1998) 1.
- [8] R. Rapp, nucl-th/9804065.
- [9] J. V. Steele, H. Yamagishi, and I. Zahed, Phys. Rev. **D56** (1997) 5605; Nucl. Phys. **A638** (1998) 495c.
- [10] P. Huovinen and M. Prakash, nucl-th/9812028.
- [11] H. Yamagishi and I. Zahed, Ann. Phys. **247** (1996) 292.
- [12] L. D. McLerran and T. Toimela, Phys. Rev. **D31** (1985) 545;
H. A. Weldon, Phys. Rev. **D42** (1990) 2384.
- [13] Particle Data Group, Phys. Rev. **D50** (1994) 1341.
- [14] V. Bernard, N. Kaiser, and U.-G. Meissner, Nucl. Phys. **B373** (1992) 346.
- [15] A. Lepretre *et al.*, Phys. Lett. **B79** (1978) 43;
J. Ahrens, Nucl. Phys. **A446** (1985) 229c;
J. Ahrens *et al.*, Phys. Lett. **B146** (1984) 303;
Th. Frommhold *et al.*, Phys. Lett. **B295** (1992) 29; Zeit. Phys. **A350** (1994) 249;
N. Bianchi *et al.*, Phys. Lett. **B299** (1993) 219; Phys. Rev. **C54** (1996) 1688.
- [16] G. Q. Li, C. M. Ko, and G. E. Brown, Nucl. Phys. **A606** (1996) 568;
E. L. Bratkovskaya and W. Cassing, Nucl. Phys. **A619** (1997) 413.
- [17] R. Rapp and J. Wambach, in preparation.